

Surface Hydrogen Incorporation and Profile Broadening Caused by Sheath Expansion in Hydrogen Plasma Immersion Ion Implantation

Zhineng Fan, Xuchu Zeng, *Member, IEEE*, Dixon Tat-Kun Kwok, *Member, IEEE*, and Paul K. Chu, *Senior Member, IEEE*

Abstract—Hydrogen plasma immersion ion implantation (PIII) in conjunction with ion-cut is an efficient and economical technique to synthesize silicon-on-insulator (SOI) substrates. Unlike beam-line ion implantation, the PIII hydrogen profile usually exhibits multiple peaks because of different implanted species, such as H^+ , H_2^+ , and H_3^+ . In addition, a certain amount of adsorbed hydrogen exists near the surface and the hydrogen in-depth distribution is broader than that of a beam-line implant also as a result of a low-energy component. For the ion-cut process, the broadened hydrogen profile and surface hydrogen can decrease the efficiency of the blistering process, induce uneven exfoliation, and degrade the interfacial quality of the bonded wafer. Hydrogen can adsorb on the wafer surface during the “off-cycle” of the sample voltage pulse and consequently be driven in by ion mixing or diffusion. In order to reduce surface hydrogen incorporation, the implantation time must be short, and this requires an efficient cooling mechanism on the sample stage because a high ion current is needed to implant a high dose in a short time (less than 5 min). Another mechanism of profile broadening is that the expanding sheath creates low-energy ions during PIII. Our experimental and simulation data disclose that profile broadening is less severe for a shorter sample voltage pulsewidth and that good blistering characteristics can be achieved using a long pulse, in spite of a relatively long implantation time of 1 h.

Index Terms—Ion-cut, plasma immersion ion implantation (PIII), silicon-on-insulator (SOI).

I. INTRODUCTION

SILICON-ON-INSULATOR (SOI) is a desirable substrate to fabricate low-power, low-voltage microelectronics devices [1], [2]. The two mainstream techniques are separation by implantation of oxygen (SIMOX) and bonding-and-etching SOI (BESOI). Bruel *et al.* recently demonstrated that SOI wafers could be produced using a layer transfer technique encompassing hydrogen implantation, wafer bonding, and cleavage [3], and this process has attracted much attention [4], [5]. Plasma immersion ion implantation (PIII) has been proposed to be an alternative to conventional beam-line ion implantation in this ion-cut process [6], [7]. PIII is an efficient and economical approach to implant a high dose of hydrogen

into a silicon wafer, and as the implantation time is independent of the wafer diameter, it is more appealing for larger wafers. However, PIII has a practical voltage limit of about 100 kV and is not the preferred technique to make thick SOI substrates for power devices, but for fully depleted complementary metal oxide silicon (CMOS) devices requiring thin SOI, PIII ion-cut is indeed attractive [8]–[10].

In a typical PIII ion-cut process, the wafer is immersed in a hydrogen plasma and pulsed biased to a negative voltage to initiate ion implantation. Depending on the plasma density, the implantation current can be high (>1 A). Because the whole wafer is implanted simultaneously, the energy deposited onto the wafer can be on the order of several kilowatts. Without careful control of the experimental conditions, such as sample cooling, the sample can get very hot and even melt. For instance, in the DC mode, 5-min hydrogen implantation at 40 kV can heat the sample up to 500 °C, a temperature high enough to cause premature exfoliation during the implantation process. For the ion-cut process, the silicon wafer must be implanted at less than 300 °C to retain the implanted hydrogen and avoid surface blistering [8]. Therefore, the preferred operating mode is pulsed PIII as the pulsing frequency can be reduced to allay wafer heating, unless an extremely efficient sample cooling mechanism is implemented.

SOI wafers up to 200 mm in diameter have been successfully fabricated using PIII ion cut. However, the implanted hydrogen profile as revealed by secondary ion mass spectrometry (SIMS) does not show a distribution resembling that of a beam-line implant. A high surface hydrogen concentration exists, and the hydrogen in-depth distribution is broader, sometimes extending from the near-surface region to the projected range of H_2^+ (H^+ population is negligible in our system [11]) if a large quantity of H_2^+ and H_3^+ coexists in the plasma. As the entire wafer is immersed in a hydrogen plasma during PIII, hydrogen atoms can adsorb onto the wafer surface during the “off-cycle” of the voltage pulse and subsequently diffuse or be knocked into the substrate by ion mixing. If this surface hydrogen concentration is high, it can impede wafer bonding and leaves patches of voids on the SOI or acceptor wafer. Another cause of the broadening in the hydrogen profile is the sheath expansion at the beginning of each pulse. When a negative pulse is applied to the wafer, electrons are repelled on the time scale of 10^{-10} s and a plasma sheath is formed. The sheath continues to expand and ions are brought in motion on the time scale of 10^{-7} s. The time to achieve a static Child law sheath state is on the order of 10 ns

Manuscript received April 28, 1999; revised December 1, 1999. The work was supported by the City University of Hong Kong, under Grant 7000964, and the Hong Kong Research Grants Council, under earmarked Grants 9040332, 9040344, and 9040412.

The authors are with the Department of Physics and Materials Science, City University of Hong Kong, Kowloon, Hong Kong (e-mail: paul.chu@cityu.edu.hk).

Publisher Item Identifier S 0093-3813(00)03662-6.

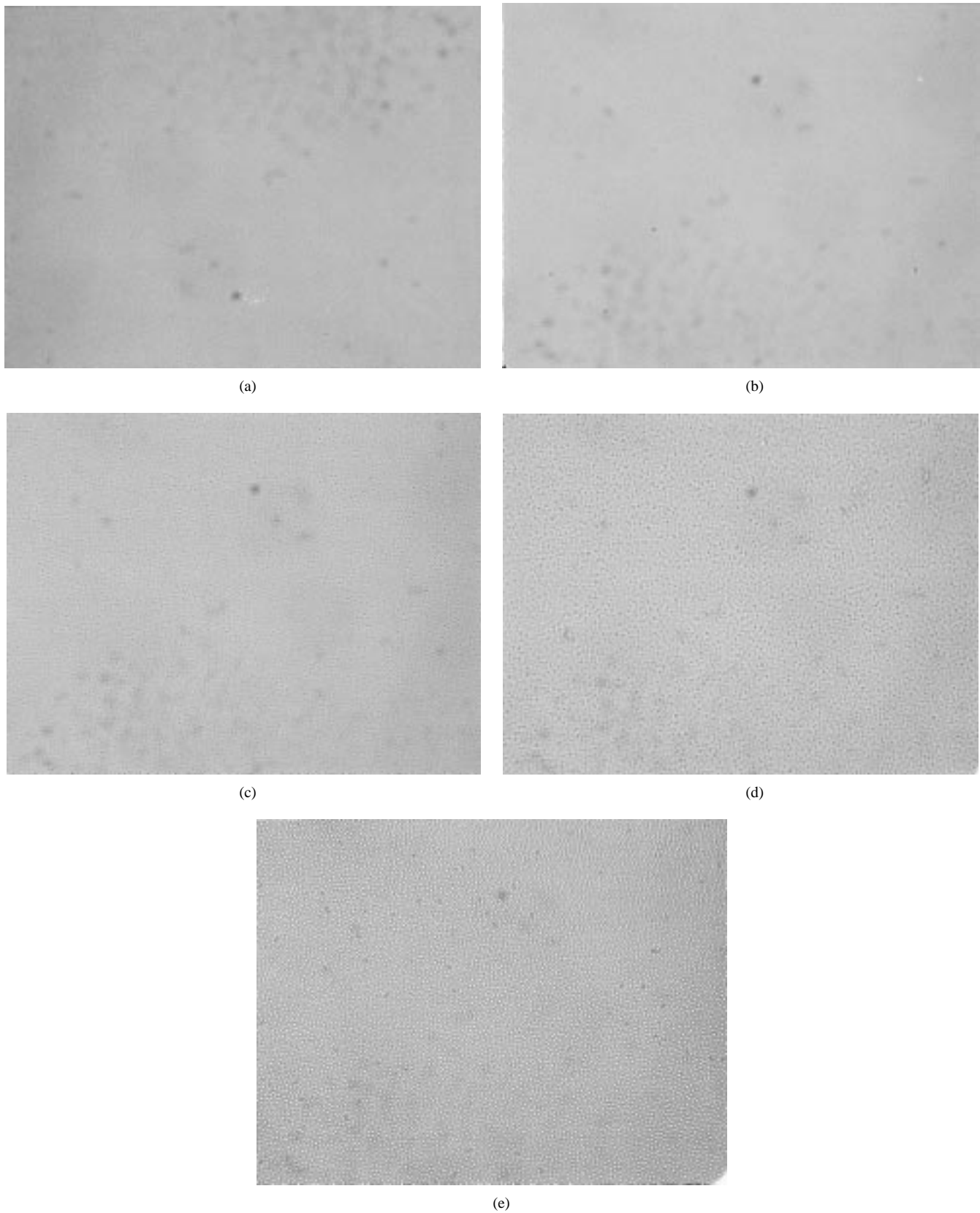


Fig. 1. Surface morphologies (500x optical micrographs) of the heat-treated samples implanted using five different pulsewidths: (a) 5 μ s, (b) 10 μ s, (c) 30 μ s, (d) 60 μ s, and (e) 100 μ s.

or longer. Because the sheath propagation is much slower than ion movement, this period can be described by the quasistatic Child law [12]. Although the ions in the quasistatic Child law

sheath are implanted at a voltage almost equal to the applied voltage, the ions in the sheath, especially those in the vicinity of the sample surface, are implanted at a lower energy. The lowest

energy can be near zero if the initial position of the hydrogen ion is just above the wafer at the beginning of the pulse. In this work, silicon wafers are implanted using different pulsewidths and annealed to cause blistering. The samples implanted using a longer pulsewidth are observed to show better blistering efficacy. The results can be explained by a reduction of the low-energy component in a long pulse mode and supported by secondary ion mass spectrometry (SIMS) and simulation data.

II. EXPERIMENTAL

Hydrogen PIII experiments were conducted in our semiconductor PIII machine [14] employing five pulse durations: 5, 10, 30, 60, and 100 μs . P-type, 100-mm, 10–20 $\Omega\text{-cm}$, $\langle 100 \rangle$ silicon wafers were implanted. The RF power was 300 W, working pressure was 4×10^{-4} torr, and implantation voltage was 20 kV. In order to isolate the effects of the sheath expansion, that is, keeping the amount of adsorbed hydrogen constant, the implantation time was the same for all samples (1 h). The pulsing frequency for each run was adjusted to maintain the same integrated current for all samples. The nominal implantation dose was 5×10^{16} atoms/cm². The voltage and current waveforms were similar to the ones reported in our other paper [15]. After implantation, the samples were annealed at 600 °C for 5 min to assess the blistering efficacy.

III. SIMULATION

We employ a one-dimensional (1-D) particle-in-cell method [16] to simulate the energy distribution of the implanted ions at pulse durations of 10, 60, and 100 μs . The rise time and fall time of each pulse used in the simulation are based on the experimental waveforms of our modulator and are 1 μs and 3 μs , respectively [15]. The plasma consists mainly of H_3^+ ions [10], [11], [15]. The plasma density is 1.0×10^9 cm⁻³, and “noncollisional” conditions are satisfied because of the low-working gas pressure. The applied voltage is –20 kV. The potential, ϕ , is related to the ion density, n_i , and electron density, n_e , by Poisson's equation

$$\nabla^2 \phi = -\frac{(n_i - n_e)}{\epsilon_0} \quad (1)$$

where ϵ_0 is the dielectric constant. The electron temperature T_e is 2 eV, and n_e is given by Boltzmann's function

$$n_e = n_o \exp\left(\frac{q\phi}{T_e}\right) \quad (2)$$

where q is the elemental charge. The potential, ϕ , is solved by (1) and finite difference. The acceleration a , initial velocity v_i , final velocity v_f , and displacement x of each ion within a time step Δt is obtained by Newton's equations

$$v_f = v_i + a\Delta t \quad (3a)$$

$$x = v_i\Delta t + \frac{1}{2}a(\Delta t)^2. \quad (3b)$$

A total of 40 000 particles are used in the simulation. Each particle represents 3.75×10^6 cm⁻² density. The grid spacing is 0.75 cm and the time step is 3.5×10^{-3} μs .

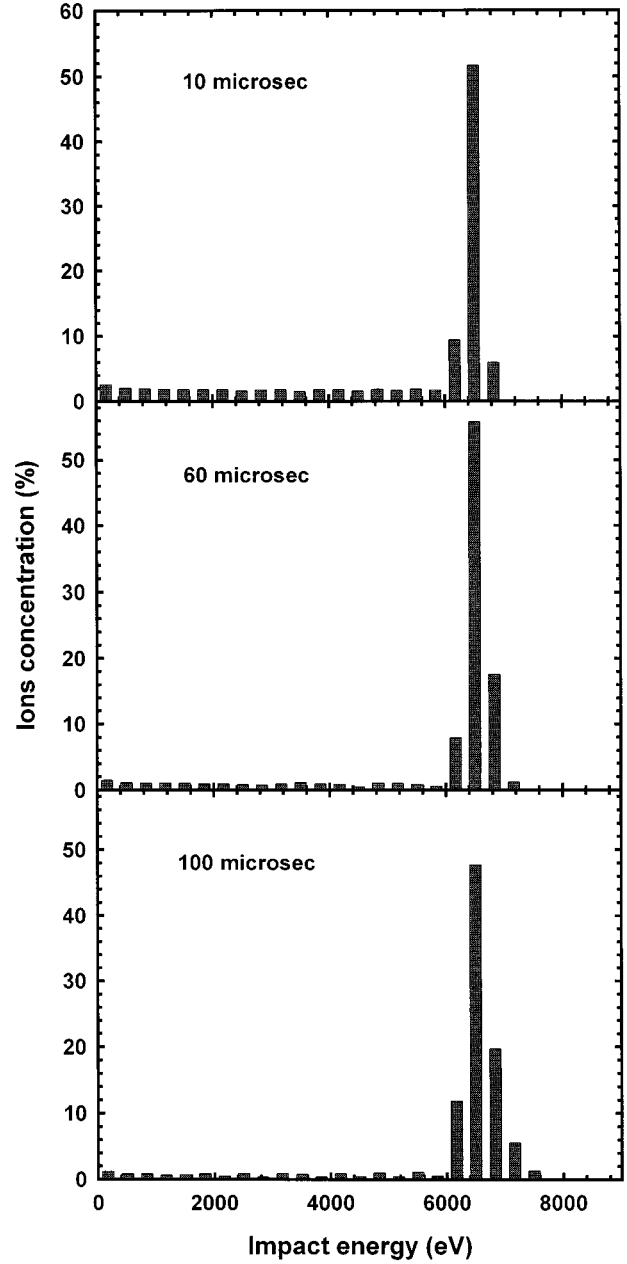


Fig. 2. Histogram of the theoretical energy distribution of the implanted hydrogen ions at 10-, 60-, and 100- μs pulsewidths.

IV. RESULTS AND DISCUSSION

Bubble formation is the basic phenomenon inducing layer cleavage in the ion-cut technique. Coalescence of the bubbles or microcavities along the peak of the implant distribution creates a structurally weakened plane parallel to the wafer surface. If the implanted wafer (a donor wafer in ion-cut terminology) is bonded to another wafer (an acceptor wafer), layer cleavage occurs along the weakened plane in the donor wafer and the detached film is transferred to the acceptor wafer. In the absence of a stiffener or bonded wafer on the implanted wafer, bubble formation leads to surface blistering, which is visible under an optical microscope and sometimes to the naked eyes. The bubble density and size provide a quick, albeit indirect, manifestation of the effectiveness of the exfoliation process. That is, a denser

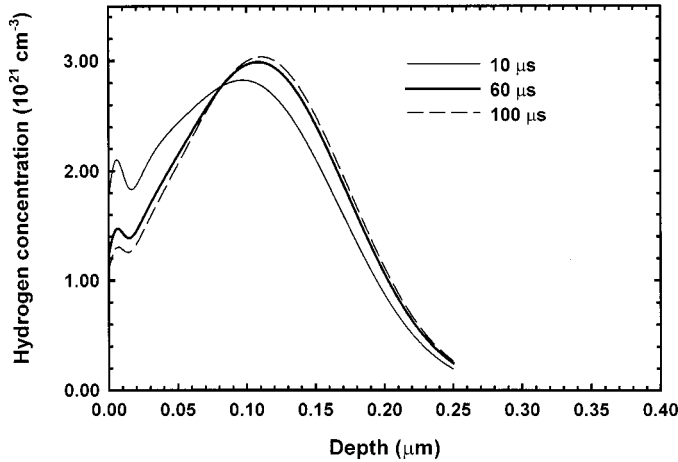


Fig. 3. Simulated hydrogen depth profiles of samples implanted using 10-, 60-, and 100- μ s pulse durations.

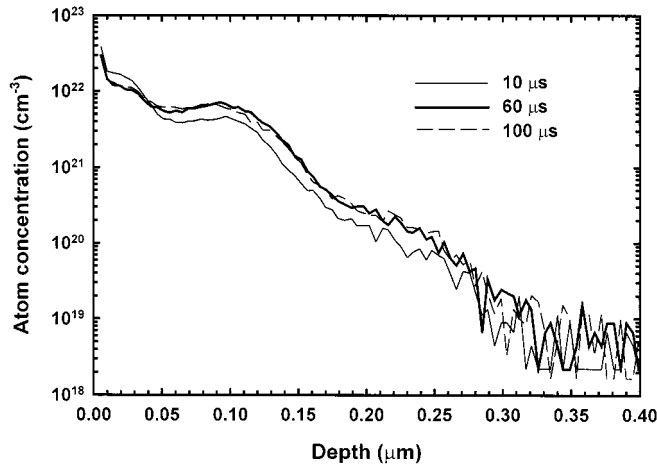


Fig. 4. SIMS depth profiles of the three silicon samples implanted using pulsewidths of 10-, 60-, and 100- μ s.

bubble distribution and bigger bubbles give rise to more effective cleavage and layer transfer in the ion-cut process. Fig. 1 depicts the optical pictures of the five silicon samples implanted using five different pulsewidths and, subsequently, heated to cause spontaneous blistering. Bubbles cannot be observed on the samples implanted using a pulse width of 5 μ s [Fig. 1(a)] and 10 μ s [Fig. 1(b)], whereas the sample implanted using 100 μ s pulse width [Fig. 1(e)] displays the biggest bubbles and highest density. The bubbles on the other two samples [30 μ s in Fig. 1(c) and 60 μ s in Fig. 1(d)] are smaller than those in Fig. 1(e), with Fig. 1(c) showing smaller and not as many bubbles. As the implant dose is nominally the same (verified by SIMS; see Fig. 4), the phenomenon cannot be explained by a dose effect. It must stem from a difference in the implanted hydrogen distribution as a result of the different pulsewidths.

The blistering observation is consistent with the cracking temperature observed for the bonded structures. The samples implanted employing 30- μ s and 60- μ s pulses were bonded to a silicon wafer with a pregrown 150-nm thermal oxide layer. The bonded structures were then annealed to achieve layer transfer. The cracking temperature could be identified by a clear sound when the structure cleaved. The cracking

temperature was 600 $^{\circ}$ C and 500 $^{\circ}$ C for the 30- μ s and 60- μ s samples, respectively.

Fig. 2 displays the histogram of the simulated energy distribution of the implanted hydrogen. It shows that the contribution of low-energy hydrogen is higher for a shorter pulsewidth. These low-energy ions are implanted mainly during the rise and fall of each negative pulse. Based on our simulation, the relative concentration of low-energy ions (below 6 keV) is 33% for a 10- μ s pulse. It drops to 17.2% for 60- μ s pulses and 13.7% for 100- μ s pulses. For a longer pulsewidth, the ratio of the rise and fall time to the total pulse duration is smaller, and the relative portion of these low-energy ions is consequently lower.

The simulated hydrogen depth profiles at pulsewidths of 10 μ s, 60 μ s, and 100 μ s are depicted in Fig. 3. Each depth profile is calculated by summing the weighted contributions at different energies according to Fig. 2. Using a Gaussian implant distribution, the total dose is

$$N(x) = \sum N_i(x) = \sum \frac{d_i}{\sqrt{2\pi}\Delta R_p} \exp\left[-\frac{(x-R_p)^2}{2\Delta R_p^2}\right] \quad (4)$$

where $N_i(x)$, d_i , R_p , and ΔR_p are the concentration, dose, projected range, and standard deviation, respectively, for each implant energy. The sum of d_i is equal to 5×10^{16} cm^{-2} . The TRIM code [17] is employed to obtain the projected range, R_p , and standard deviation, ΔR_p , at each implant energy. Fig. 3 illustrates that the 10- μ s profile is broader than those of the 60- μ s and 100- μ s, and the 10- μ s sample has more hydrogen on the surface. The difference between the 10- μ s and 60- μ s samples is bigger than that between the 60- μ s and 100- μ s samples, because a 500% increase occurred in the pulsewidth from 10- μ s to 60- μ s, whereas the relative increase is only 67% going from 60 μ s to 100 μ s. A broader distribution at the same implant dose results in a lower hydrogen peak concentration reducing the bubble density and consequently the cracking efficacy, as illustrated by our cracking experiments. The higher surface hydrogen observed for the 10- μ s sample may also diminish the blistering effectiveness and lead to more bonding voids in the ion-cut process.

To verify the simulation results, the samples were analyzed by high depth resolution SIMS, and the hydrogen depth profiles of the 10-, 60-, and 100- μ s samples are exhibited in Fig. 4. The SIMS data are qualitatively in line with our theoretical calculation, with the 10- μ s pulsewidth hydrogen profile exhibiting discernible higher surface hydrogen component and lower peak hydrogen concentration than the 60- μ s and 100- μ s samples. However, it should be noted that our simulation does not take into account surface hydrogen adsorption during the PIII process, particularly during the “off-cycle” period of the high voltage pulse, which is much longer than the “on-cycle” period because of the low duty cycle used in this work to keep the sample temperature low. On the other hand, both of these effects are manifested in the SIMS profiles, and comparing Figs. 3 and 4, neutral hydrogen adsorption onto the silicon surface during the PIII process is severe. No easy way exists to simulate neutral hydrogen adsorption because it depends on the plasma and surface chemistry, and so it is very difficult to match the theoretical and

experimental data (from surface to about 0.04- μm , according to the SIMS data) perfectly. Experimentally, the amount of adsorbed hydrogen can be reduced only by shortening the total exposure or implantation time. This reduction can be achieved by using a higher plasma density or higher pulsing frequency, both of which requiring more efficient sample cooling.

Our theoretical and experimental results indicate that long pulse PIII gives rise to a smaller amount of low-energy hydrogen ions and, consequently, better blistering characteristics. For PIII ion-cut, a long pulse is thus preferred. However, in practice, it is more difficult to maintain stable plasma in a long pulse mode because the plasma sheath may propagate to the vacuum chamber wall [15]. Hence, long pulse PIII demands better hardware, such as a larger chamber and higher power RF source (to create a higher density plasma and thinner sheath), but it should be noted that more efficient sample cooling will be needed if the plasma density is high.

V. CONCLUSION

Silicon wafers implanted by hydrogen PIII using a longer pulsewidth show better blistering characteristics. Our simulation and experimental results indicate that it is caused by a decrease in the relative amount of the low-energy hydrogen component broadening the hydrogen depth profile and reduces the peak hydrogen concentration. Therefore, a long pulsewidth is preferred for the hydrogen PIII/ion-cut process, even though better hardware is required.

REFERENCES

- [1] S. Cristoloveanu and S. S. Li, *Electrical Characterization of Silicon-On-Insulator Materials and Devices*. Boston, MA: Kluwer Academic Publishers, 1995.
- [2] J. P. Colinge, *Silicon-on-Insulator Technology: Materials to VLSI*, 2nd ed. Boston, MA: Kluwer Academic Publishers, 1997.
- [3] M. Bruel, B. Aspar, B. Charlet, C. Maleville, T. Poumeyrol, A. Soubie, A. J. Auberton-Herve, J. M. Lamure, T. Barge, F. Metral, and S. Trucchi, "Smart-cut[®]: A promising new SOI material technology," in *Proc. 1995 IEEE Int. SOI Conf.*, Tucson, AZ, 1995, pp. 178–179.
- [4] Q. Y. Tong, T. H. Lee, K. Gutiahr, S. Hopfe, and U. Gosele, "Layer splitting process in hydrogen-implanted Si, Ge, SiC and diamond substrate," *Appl. Phys. Lett.*, vol. 70, pp. 1390–1392, 1997.
- [5] L. B. Freund, "A lower bond on implant density to induce wafer splitting in forming compliant substrate structures," *Appl. Phys. Lett.*, vol. 70, pp. 3519–3521, 1997.
- [6] J. R. Conrad, J. L. Radtke, R. A. Dodd, F. J. Worzala, and N. C. Tran, "Plasma source ion-implantation technique for surface modification of materials," *J. Appl. Phys.*, vol. 62, pp. 4591–4596, 1987.
- [7] P. K. Chu, S. Qin, C. Chan, N. W. Cheung, and L. A. Larson, "Plasma immersion ion implantation—A fledgling technique for semiconductor processing," *Mat. Sci. Eng.: Rep.*, vol. R17, pp. 207–280, 1996.
- [8] X. Lu, N. W. Cheung, M. D. Strathman, P. K. Chu, and B. Doyle, "Hydrogen induced silicon surface layer cleavage," *Appl. Phys. Lett.*, vol. 71, pp. 1804–1806, 1997.
- [9] X. Lu, S. S. K. Iyer, C. Hu, N. W. Cheung, J. Min, Z. Fan, and P. K. Chu, "Ion-cut silicon-on-insulator fabrication with plasma immersion ion implantation," *Appl. Phys. Lett.*, vol. 71, pp. 2767–2769, 1997.
- [10] Z. Fan, "SOI synthesis by plasma immersion ion implantation," Ph.D. dissertation, City University of Hong Kong, Hong Kong, 1998.
- [11] P. K. Chu and N. W. Cheung, "Microcavity engineering by plasma immersion ion implantation," *Mater. Chem. and Phys.*, vol. 57, pp. 1–16, 1998.
- [12] M. A. Lieberman, "Model of plasma immersion ion implantation," *J. Appl. Phys.*, vol. 66, pp. 2926–2929, 1989.
- [13] J. R. Conrad, "Sheath thickness and potential profiles of ion-matrix sheath for cylindrical and spherical electrons," *J. Appl. Phys.*, vol. 62, pp. 777–779, 1987.

- [14] P. K. Chu, S. Qin, C. Chan, N. W. Cheung, and P. K. Ko, "Instrumental and process considerations for the fabrication of silicon-on-insulators (SOI) structures by plasma immersion ion implantation," *IEEE Trans. Plasma Sci.*, vol. 26, no. 6, pp. 79–84, 1998.
- [15] Z. Fan, Q. Chen, P. K. Chu, and C. Chan, "Low pressure plasma immersion ion implantation of silicon," *IEEE Trans. Plasma Sci.*, vol. 26, pp. 1661–1668, Dec. 1998.
- [16] D. T.-K. Kwok, P. K. Chu, and C. Chan, "Ion dose uniformity for planar sample plasma immersion ion implantation," *IEEE Trans. Plasma Sci.*, vol. 26, no. 6, pp. 1669–1679, 1998.
- [17] J. F. Ziegler, J. P. Biersack, and U. Littmark, *The Stopping and Range of Ions in Solids*. New York, NY: Pergamon, 1985.



Zhineng Fan received the B.S. degree in physics and the M.S. degree in materials science from Fudan University, Shanghai, People's Republic of China, in 1992 and 1996, respectively, and the Ph.D. degree from the City University of Hong Kong, Hong Kong SAR, in 1998.

He is currently a Postdoctoral Associate at Cornell University, Ithaca, NY. His research interests include plasma immersion ion implantation, separation by plasma implantation of oxygen, ion-cut, electro-migration, and related failure mechanism.



Xuchu Zeng (M'97) was born in Sichuan, China, on February 12, 1964. He received the B.S. degree in electrical engineering from Xian JiaoTong University, China, in 1985 and the M.S. degree in plasma physics from the Southwestern Institute of Physics, China, in 1991. He is currently a Ph.D. candidate in the City University of Hong Kong.

He was Assistant Engineer, Engineer, and Senior Engineer in 1986, 1992, and 1994, respectively, in Southwestern Institute of Physics. From June 1995 to June 1997, he was a Research Staff Member of

the Plasma Laboratory of the City University of Hong Kong. His research interests include plasma immersion ion implantation equipment design as well as applications.



Dixon Tat-Kun Kwok (M'98) received the B.Sc. degree in physics in 1988 and the Ph.D. degree in solid state physics in 1993 from King's College London, University of London.

He served as a Postdoctoral Fellow until 1995 at the Surface Physics Laboratory of Fudan University in Shanghai. In April 1995 he became a Research Associate of the Physics Department of the Hong Kong University of Science and Technology in Hong Kong. He has been a Research Fellow since 1996 in the Department of Physics and Material Science of the City University of Hong Kong. He has published papers on topics related to photoluminescence and photoabsorption of point defects in silicon, reflectance difference spectroscopy, and numerical simulation of plasma immersion ion implantation.



Paul K. Chu (M'97–SM'99) received the B.S. degree in mathematics from the Ohio State University in 1977 and the M.S. and Ph.D. degrees in chemistry from Cornell University, Ithaca, NY, in 1979 and 1982, respectively.

He joined Charles Evans & Associates in California in 1982 and assumed various technical and managerial positions. He founded Evans Asia in early 1990 and later joined the City University of Hong Kong as a visiting faculty member. He is currently a Professor in the Department of Physics and Materials Science in the City University of Hong Kong, and holds concurrent professorship at Fudan University, Peking University, Southwest Jiaotong University, and Southwestern Institute of Physics in China. His research activities include plasma processing technology, semiconductor processing, and materials characterization.

Dr. Chu is a member of the American Chemical Society, Materials Research Society, TMS, and Böhmische Physical Society. He is also a Fellow of the Hong Kong Institution of Engineers.